Hindawi Publishing Corporation
Journal of Nanomaterials
Volume 2015, Article ID 905259, 10 pages
http://dx.doi.org/10.1155/2015/905259

Research Article

Efficient Degradation of Methylene Blue over Two-Dimensional Au/TiO_2 Nanosheet Films with Overlapped Light Harvesting Nanostructures

Yihan Chen, Juanjuan Bian, Lulu Qi, Enzhou Liu, and Jun Fan

School of Chemical Engineering, Northwest University, Xi'an 710069, China

Correspondence should be addressed to Enzhou Liu; liuenzhou@nwu.edu.cn

Received 26 March 2015; Accepted 17 May 2015

Academic Editor: P. Davide Cozzoli

Two-dimensional TiO_2 nanosheet films with visible light trapping nanostructures were successfully fabricated by alkali hydrothermal reaction using Ti sheet as precursor. Metallic Au nanoparticles (NPs) were then deposited on the surface of TiO_2 film through a microwave-assisted reduction process. The investigations reveal that the localized surface plasmon resonance (LSPR) of Au NPs is greatly enhanced by the overlapped light harvesting nanostructures between TiO_2 film and Au NPs, resulting in an enhanced LSPR-absorption with two peaks at 389 nm and 540 nm. The photocatalytic performance of the samples was evaluated by degradation of methylene blue (MB) as a model pollutant. The experimental results indicate that the photocatalytic performance of TiO_2 is greatly promoted by a synergetic effect between the overlapped light harvesting nanostructures and the improved charge carrier separation processes. The MB degradation over the optimal sample is much faster than that of pure TiO_2 film by a factor of 3.0 and 5.7 under UV light and UV + visible light irradiation, respectively. This study provides a simple strategy to develop film-shaped plasmonic photocatalysts with high efficiency.

1. Introduction

Since the discovery of hydrogen evolution by photoinduced water splitting over TiO_2 electrode [1], semiconductor-based photocatalysis has attracted great attention in the field of solar energy conversion and environment remediation [2–9], and considerable efforts have been dedicated to the design of various semiconductor photocatalysts with improved performance. TiO_2-based semiconductors with good chemical stability and environmental-friendly features have received far more attention in the field of photocatalytic water splitting, reduction of CO_2 with H_2O to form hydrocarbon fuels, and wastewater treatment by photodegradation of organic pollutants [10–15]. However, its utilization is negatively affected by the high recombination probability of photoexcited electron-hole pairs and its relatively large band gap (Eg = 3.2 eV). The latter makes TiO_2 without visible light ($\lambda > 400$ nm) activity, resulting in a poor solar energy utilization. As a consequence, intense research activities have been devoted to the development of visible light active TiO_2 with high photocatalytic efficiency, such as surface photosensitization, element doping, semiconductor combination, and structural control [16–28].

In 2008, Awazu et al. observed that the photocatalytic behavior of TiO_2 was greatly boosted by the localized surface plasmon resonance (LSPR) of Ag NPs during photocatalytic decomposition of methylene blue (MB) [29]. The enhancement is attributed to the enhanced near-field amplitudes of LSPR from Ag NPs. This enhanced near field could boost the excitation of electron-hole pairs in TiO_2 and result in an improved photocatalytic activity. It immediately sparked a surge of research into plasmonic photocatalysis, especially noble Ag and Au contained systems [30–38]. Further investigations reveal that the localized surface plasmonic resonance and the Schottky junction are two prominent features of plasmonic metal/semiconductor composites [39]. The former contributes to the strong absorption of visible light and the excitation of active charge carriers, whereas the latter facilitates charge separation and transfer, and they work together to achieve higher photocatalytic efficiency.

Although much work has been done to investigate LSPR-enhanced photocatalysis, the enhancement mechanism is still under debate. Jose et al. observed that the localized electric field created by Au NPs could not induce charge carriers in the near-surface region of TiO_2, because the LSPR-absorption of Au NPs does not overlap with the TiO_2 absorption [40]. The LSPR-absorption band of Au NPs is usually larger than 500 nm, and the overlap between the absorption of TiO_2 and LSPR-absorption of Au NPs is very weak, leading to a relative poor photocatalytic activity. Ingram et al. observed that N-doping could improve the optical overlap between TiO_2 and Ag NPs, and Ag-loaded N-TiO_2 composite exhibited much higher visible activity [41, 42]. Later, an enhanced photocurrent in a thin-film iron oxide photoanode coated on arrays of Au nanopillars was observed by Gao et al. [43]. The enhancement was attributed primarily to the increased optical absorption originating from both surface plasmon resonances and photonic-mode light trapping in the nanostructured topography. Their study provides an applicable solution to concentrating light in the active regions of semiconductors. In order for efficiency energy and charge transfer to take place between the metal NPs and the semiconductor photocatalyst, it is important that the spectral enhancement of the metal NPs overlaps with the spectrum absorption of the semiconductor photocatalyst. This is crucial factor for reaching maximum plasmon enhancement [41]. To the best of our knowledge, the investigation on enhanced light trapping in metal/semiconductor systems has not received much attention.

In this work, Au/TiO_2 nanosheet film was successfully fabricated through a joint hydrothermal method and microwave-assisted reduction process. This film-shaped photocatalyst can eliminate the necessity of inconvenient filtration processes required by powdered catalysts, suggesting attractive perspectives for on-site utilization. More importantly, an overlapped light harvesting phenomenon was observed in Au/TiO_2 composite film due to the unique nanostructures of TiO_2 film and LSPR of Au NPs. We found that the overlapped light harvesting nanostructures can greatly enhance the LSPR-absorption of Au NPs and improve the photocatalytic activity of Au/TiO_2 system.

2. Experiment

2.1. Preparation of Au/TiO_2 Nanosheet Films. Au/TiO_2 nanosheet films were fabricated through a joint hydrothermal method and microwave-assisted reduction process. The detailed experimental process is shown in Figure 1. First, TiO_2 film was obtained via a one-step hydrothermal method described in our previous study [44]. In detail, surface polished Ti sheet (99.5% purity, 2.1 mm × 4.2 mm × 0.5 mm) was immerged and sealed in a 100 mL Teflon-lined vessel containing NaOH aqueous solution (50 mL, 1 mol·L^{-1}) and then maintained at 180°C for 24 h. Subsequently, the sheet was cleaned with water and immerged in 0.25 wt% HCl aqueous solutions for 24 h and then washed with water again. Finally, it was annealed at 450°C for 2 h to obtain TiO_2 nanosheet film.

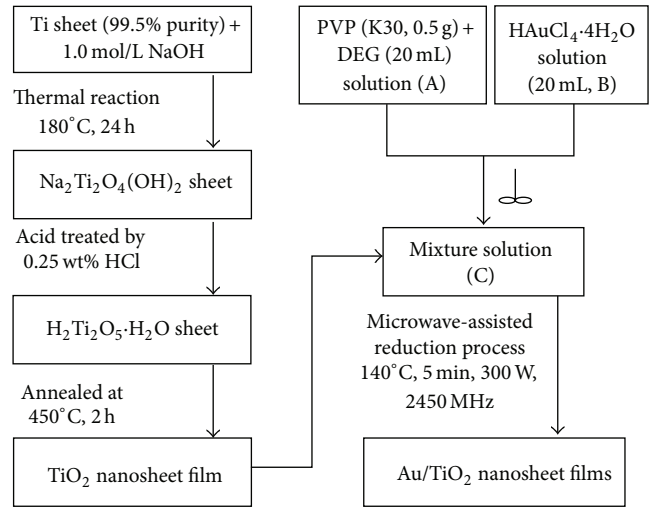

Figure 1: The detailed preparation process of Au/TiO_2 composite films.

Au NPs were deposited on the surface of TiO_2 film by a microwave-assisted reduction process in PVP-DEG solution medium inspired by Park's work [29]. First, polyvinylpyrrolidone (PVP) was dispersed in diethylene glycol (DEG) and stirred vigorously to give a transparent solution (solution A). Meanwhile, $HAuCl_4{\cdot}4H_2O$ was dissolved in water and kept stirring in dark for use (solution B). Subsequently, solution B was poured into solution A and kept stirring for 20 min to obtain solution C. Thereafter, pure TiO_2 film was immerged into the above solution C, and then they were exposed to microwave irradiation. Finally, Au/TiO_2 film was obtained after washing the sheet with water and ethanol for several times. The obtained samples were denoted as xAu/TiO_2, with x representing the millimolar concentration of Au^{3+} in reaction solution. In this work, 0.1, 0.2, 0.3, 0.4, 0.5, and 0.6 Au/TiO_2 films were prepared by changing the concentration of $HAuCl_4{\cdot}4H_2O$ precursor.

2.2. Characterizations and Photocatalytic Activity Test. The crystalline phases and morphologies of the samples were characterized by a Shimadzu XRD-6000 powder diffractometer and a scanning electron microscopy (SEM, JEOL JSM-6390A). The UV-Vis diffuse reflectance spectra were obtained on a Shimadzu UV-3600 UV/vis/NIR spectrophotometer with an integrating sphere detector, and $BaSO_4$ was used as the reflectance standard material. Besides, photoluminescence (PL) spectra were investigated on Hitachi F-7000 florescence spectrophotometer. X-ray photoelectron spectroscopy (XPS) was performed by Kratos AXIS NOVA spectrometer. Photocatalytic degradation of MB was carried out in an outer irradiation-type quartz reactor, which irradiated using a 300 W Xe-lamp (Beijing Perfectlight Technology Co. Ltd., China, Microsolar300UV, ultraviolet light: 6.6 W, visible light: 17.6 W, and the light flux about 3400 lm). Two filters were employed to achieve UV light (UVREF, $\lambda < 400$ nm) and visible light (UVCUT400, $\lambda > 400$ nm) irradiation, respectively. The system was shielded by a black box during

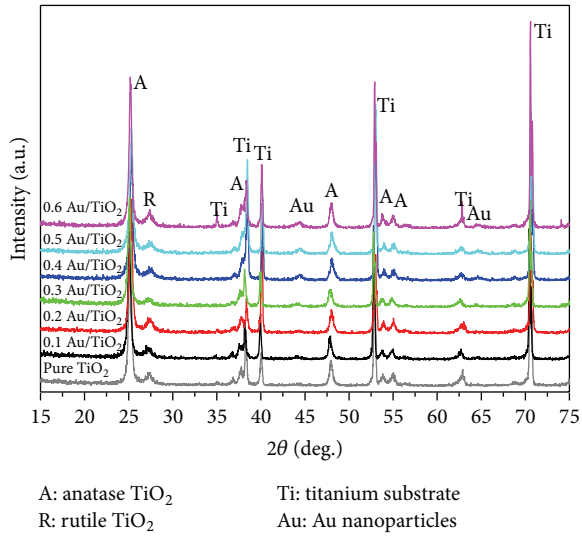

Figure 2: XRD patterns of the samples.

the reaction to prevent interference from outside light. The film was immerged in 100 mL MB aqueous solution (10 mg/L, the pH value of MB solution is about 6.3) and air was bubbled through the system continuously. It was kept in the dark for 1 h prior to irradiation for establishing adsorption-desorption equilibrium. At different times, the absorbance of MB solution was determined using a Shimadzu UV-3600 spectrophotometer. The concentration variation of MB was obtained according to the concentration-absorbance relationship (λ = 664 nm).

3. Results and Discussion

3.1. Characteristics of the Photocatalysts. The crystalline phases of the samples were investigated by XRD (Figure 2). All the peaks can be indexed using the Ti substrate (JCPDS file No: 65-6231), anatase TiO_2 (JCPDS file No: 21-1272), rutile TiO_2 (JCPDS file No: 21-1276), and metallic Au (JCPDS file number: 65-2870), respectively. The content of rutile TiO_2 is very low and it has very little effect on the UV-Vis absorption of TiO_2 (see Figure 5). Besides, the introduction of Au NPs does not affect the phase structure of TiO_2 film. The signals around 44.6° and 64.6° are attributed to metallic Au NPs, they can only be observed in the samples with a higher Au concentration. Aside from XRD analysis, the existence of Au NPs is also observed by SEM, XPS and UV-Vis investigations below (Figures 3 to 5).

Figure 3(a) presents a typical SEM image of pure TiO_2 film, which is composed by a large number of continuous distributed TiO_2 nanosheets, which are hard to detach from the Ti substrate. This is beneficial for the practical utilization of film-shaped photocatalysts. Figure 3(b) shows a typical SEM image of Au modified TiO_2 film. It can be observed that lots of spherical nanoparticles are uniformly deposited on the surface of the sheets. This two dimensional nanosheet with a rough surface can provide more active sites for the adsorption of reactant molecules, and the photogenerated charge carriers can effectively contribute to the chemical reactions on the surface. It is also worth noting that the density of Au NPs can be effectively regulated by changing the initial concentration of $HAuCl_4 \cdot 4H_2O$ according to Figures 3(c)–3(h), indicating that the microwave-assisted reduction process is a good method to deposit Au NPs. However, Au NPs with a relatively bigger size is observed when a higher concentration of $HAuCl_4 \cdot 4H_2O$ employed (Figure 3(h)).

The components and chemical status of the film were investigated by XPS. As shown in Figure 4, the signals of Ti 2p, O 1s, Au 4f and C 1S (date not shown) are detected. XPS spectrum of Ti 2p displays two peaks at 458.7 eV and 464.4 eV in Figure 4(a), they are assigned to Ti $2p_{3/2}$ and Ti $2p_{5/2}$ spin-orbit components of Ti^{4+} [45]. The signal at 530.0 eV is attributed to the lattice oxygen of TiO_2 in Figure 4(b) [46]. Figure 4(c) shows the Au 4f XPS spectrum with two peaks at 83.4 eV and 87.0 eV for Au $4f_{7/2}$ and Au $4f_{5/2}$, respectively, suggesting Au species are in metallic Au^0 state in the composites. The relative negative shift (0.6 eV) of Au $4f_{7/2}$ peak with respect to bulk Au ($4f_{7/2}$ peak at 84.0 eV) may be caused by the electron redistribution (from TiO_2 to Au) at the contact interface when their Fermi levels are aligned [47]. Further investigations reveal that the chemical state of Au NPs is maintained after the reaction (Figure 4(c)).

Figure 5 shows a comparison of UV-Vis diffuse reflection absorption spectra of P25 (a kind of widely used commercial TiO_2 photocatalyst), pure TiO_2 film and Au/TiO_2 films. Aside from an enhanced UV light absorption compared with P25, the as-prepared TiO_2 film also exhibits excellent visible light trapping property due to its unique nanostructures. It is usually attributed to the scattering of light caused by pores or cracks in the film [46, 48–50]. Those pores or cracks may function as "black hole" to trap the incident light (Figure 3(f)). The absorption of pure TiO_2 film in UV light region shows a clear absorption edge shorter than 390 nm due to the intrinsic band gap absorption of anatase TiO_2 (Eg = 3.2 eV). It is worth mentioning that the TiO_2 films loaded with Au NPs show a broad absorption in the visible region, this originates from the outstanding light trapping property of Au NPs for their LSPR effect. The absorption intensity of Au/TiO_2 films increases with increasing the initial concentration of $HAuCl_4 \cdot 4H_2O$, which can lead to more Au NPs deposited on the TiO_2 surface (Figures 3(c)–3(h)). In addition, the photographs of the samples under natural sunlight exhibits a distinct color change from gray to dark red after the loading of Au NPs (not shown here). This is in line with the UV-Vis absorption spectra of the samples in Figure 5.

3.2. Photocatalytic Activities of MB Degradation. The degradation of MB was firstly conducted under UV light and visible light irradiations without filters, the elections and holes play very important roles during the degradation. The adsorbed dye molecules can be oxidized directly due to the strong oxidizing property of active holes on the surface of catalyst. The excited electrons trapped by oxygen molecule can form $\cdot O_2^-$ and ·OH active radicals and they can also oxidize dyes. As shown in Figure 6(a), all the Au/TiO_2 films exhibit higher activity for MB degradation than for pure TiO_2 film

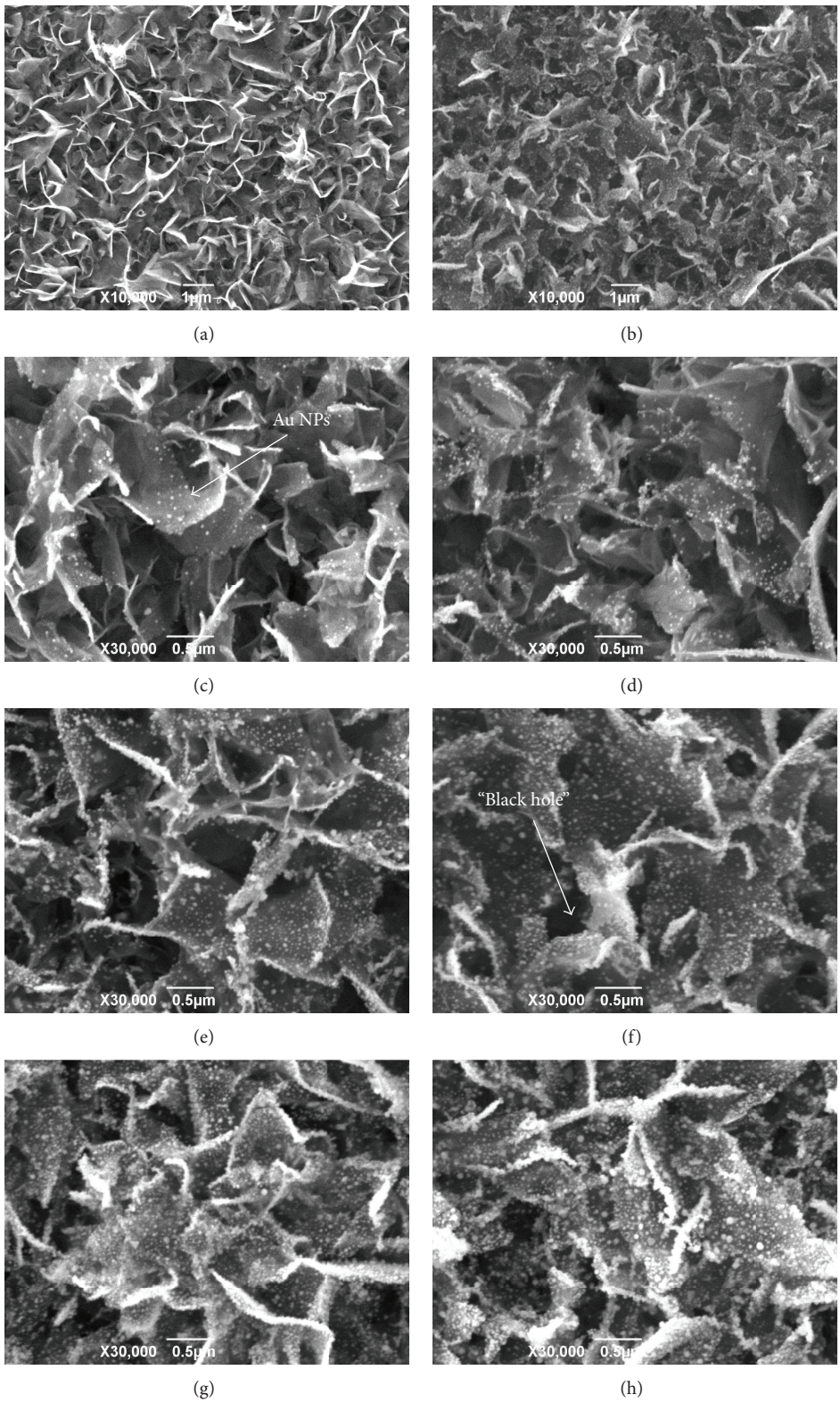

Figure 3: SEM images of (a) pure TiO_2 film, (b) Au modified TiO_2 film, and the magnification of (c) 0.1 Au/TiO_2, (d) 0.2 Au/TiO_2, (e) 0.3 Au/TiO_2, (f) 0.4 Au/TiO_2, (g) 0.5 Au/TiO_2 and (h) 0.6 Au/TiO_2 films.

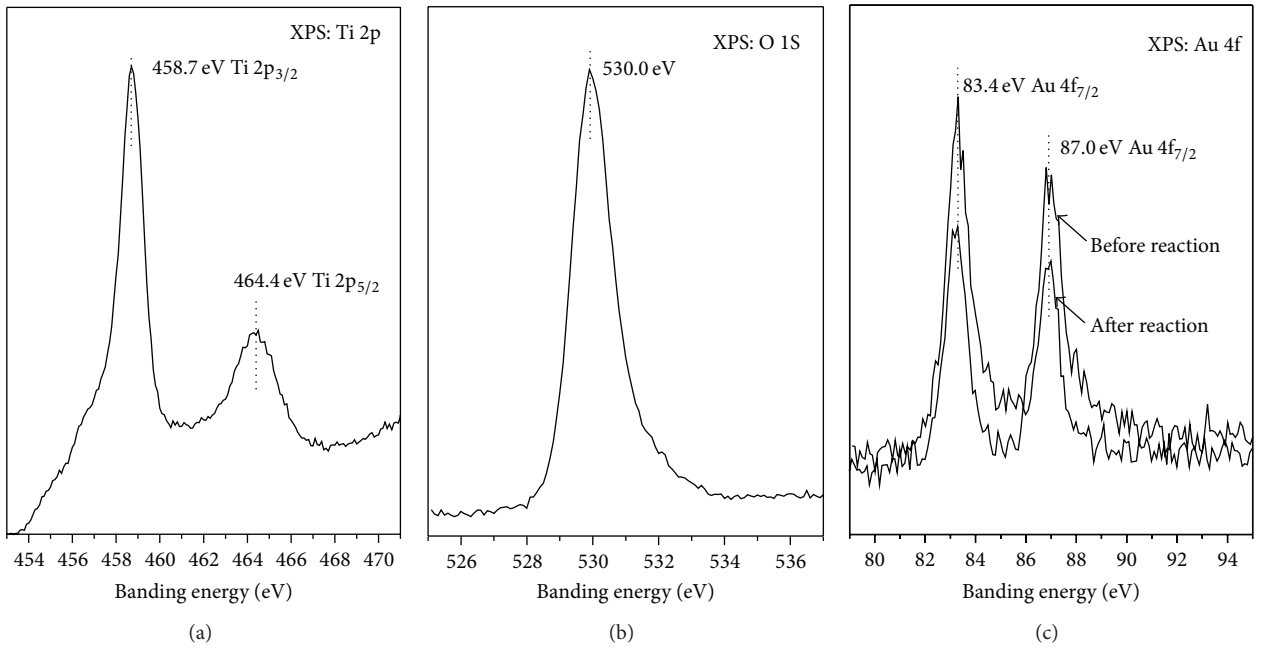

FIGURE 4: XPS spectra of Au/TiO_2 film: (a) Ti 2p, (b) O 1s, and (c) Au 4f.

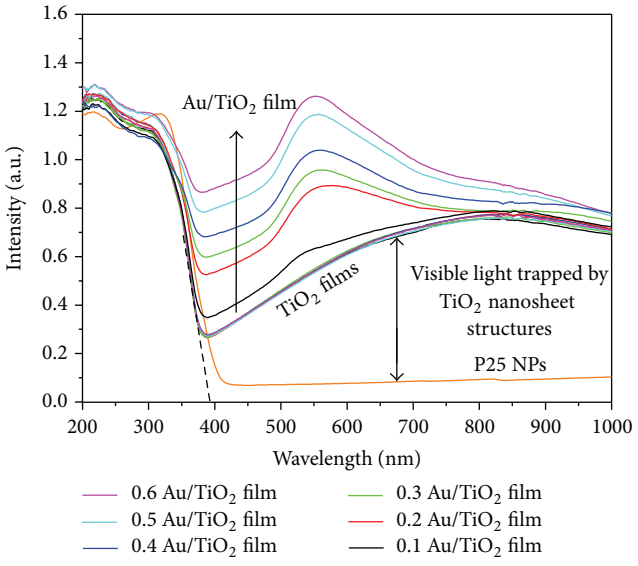

FIGURE 5: UV-Vis diffuse reflection absorption spectra of the samples, including commercial P25 TiO_2 nanoparticles, pure TiO_2 film, and Au/TiO_2 films.

(about 50% of MB is degraded), and the degradation efficiency increases with increasing the content of Au NPs, indicating that Au NPs has a great effect on the performance of TiO_2 film. However, the increase is no longer apparent when Au NPs are over deposited. The degradation percentage of MB is almost the same over 0.5 Au/TiO_2 and 0.6 Au/TiO_2 after long-term irradiation, and about 97% of MB can be degraded after 2 h irradiation. Although 0.6 Au/TiO_2 exhibits good visible light harvesting property (Figure 5), the adsorption-desorption of MB may be the rate controlling process at the end of the degradation. A pseudo-first-order kinetic model was employed to fit the degradation data by using the following equation: $-\ln(C/C_0) = kt$ (k is the kinetic constant) [13, 16, 51]. Figure 6(b) shows the degradation rate constant k of MB over different samples, and 0.6 Au/TiO_2 film shows the highest catalytic activity with a k of 0.0287 min^{-1}, about 5.7 times higher than that of pure TiO_2 film (k = 0.0050 min^{-1}).

To further reveal the roles of Au NPs, the experiment was conducted over pure TiO_2 and 0.6 Au/TiO_2 films under UV light and visible light irradiations, respectively. The experimental results are presented in Figure 7. Under UV light irradiation, 0.6 Au/TiO_2 film exhibits higher activity than that of pure TiO_2 film, the corresponding degradation percentage is 66% and 38% after 2 h of irradiation, and k of 0.6 Au/TiO_2 film is 0.0086 min^{-1}, about 3.0 times higher than that of pure TiO_2 film (k = 0.0029 min^{-1}). This is because the Schottky junction between Au and TiO_2 can facilitate charge separation. The work function of Au (Φ = 5.1 eV) is higher than anatase TiO_2 (Φ = 4.2 eV). Hence the generation probability of electrons from anatase TiO_2 under UV irradiation and their transfer to the Au NPs is high [52], and it is similar to Ag/TiO_2 systems [53–55]. The electrons transfer from the conduction band of TiO_2 to Au NPs can reduce the recombination chance of electrons and holes, facilitating the photoreaction process. It is verified by the PL spectra in Figure 8. The emission peaks around 467 nm and 397 nm are due to the radioactive recombination of photogenerated electron-hole pairs [56, 57]. Fluorescence quenching is observed after Au deposition under the excitation of 220 nm. This can be attributed to

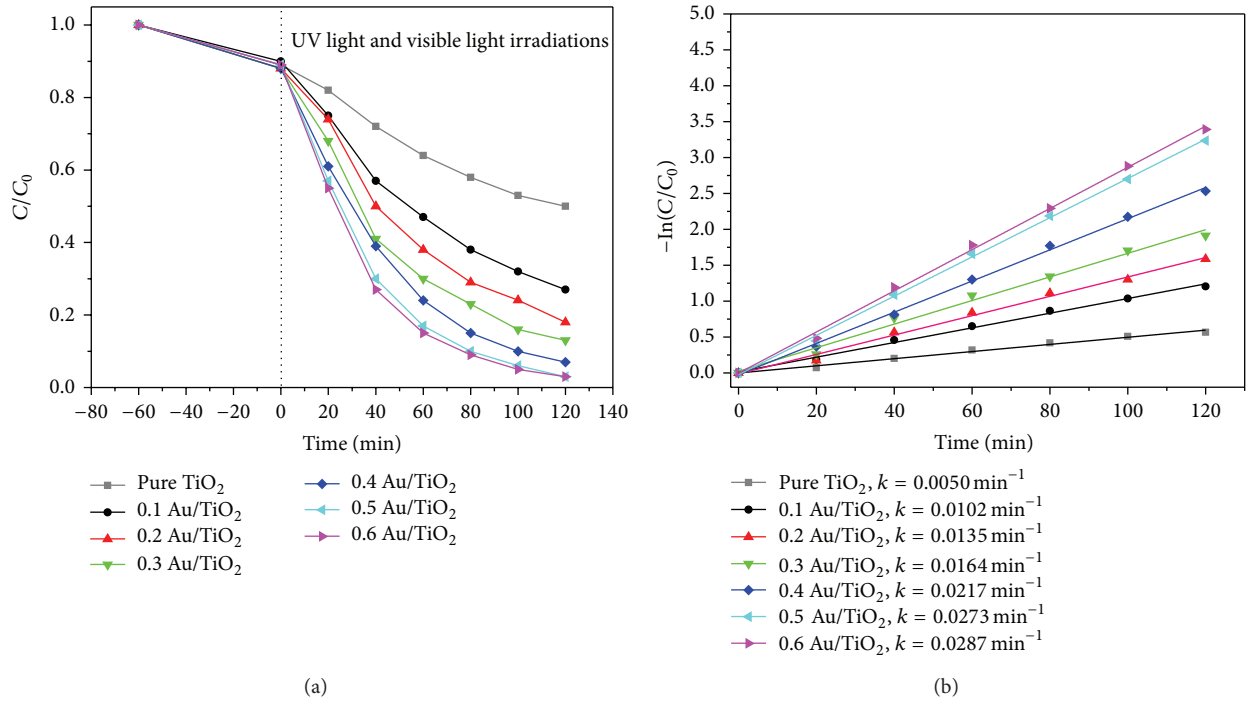

FIGURE 6: (a) The normalized concentration of MB over different samples under UV light and visible light irradiations; (b) the corresponding kinetics of MB degradation (where C is the concentration of MB at the irradiation time t and C_0 is the concentration of adsorption equilibrium with the catalyst before irradiation).

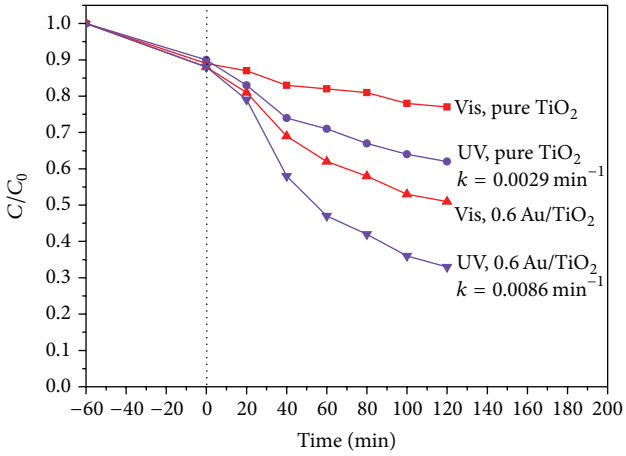

FIGURE 7: The normalized concentration of MB over pure TiO_2 and 0.6 Au/TiO_2 films under UV light irradiation and visible light irradiation, respectively.

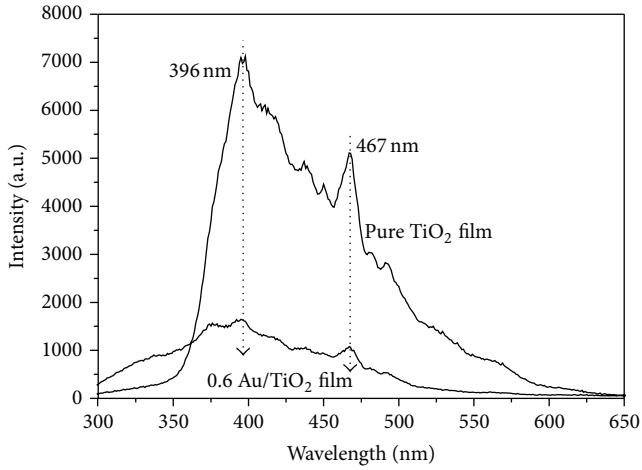

FIGURE 8: PL spectra of pure TiO_2 and 0.6 Au/TiO_2 films under the excitation of 220 nm (PMT voltage: 650 V).

the effective capture of photoexcited electrons by Au NP, leading to lower emission intensity.

Under visible light irradiation, the unique nanostructures of TiO_2 film can enhance the MB photosensitization by trapping the visible light and accelerate the degradation process, and 23% of MB is degraded over pure TiO_2 film after 2 h irradiation. Compared with the pure TiO_2 film, 0.6 Au/TiO_2 film exhibits a relatively higher photocatalytic performance and 49% of MB is degraded after 2 h irradiation. This is benefit from the overlapped visible light absorption between Au NPs and TiO_2 film. On the one hand, the MB photosensitization over pure TiO_2 film may be improved by Au NPs under visible light irradiation due to LSPR-absorption, by which the light energy can be effectively coupled into MB molecule and promote photosensitization. On the other hand, the activity of Au/TiO_2 composites under visible light may result from the LSPR effect of Au NPs. It has been proven that LSPR-absorption of Au NPs can generate plasmon induced

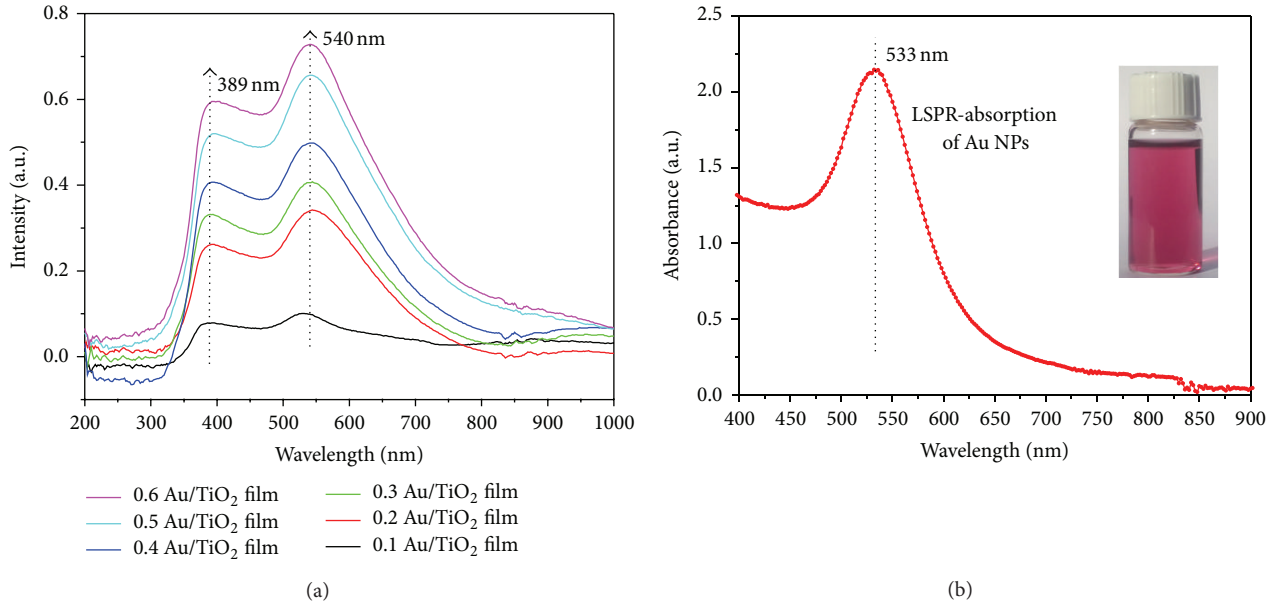

Figure 9: (a) LSPR-absorption of Au NPs in Au/TiO_2 samples; (b) LSPR-absorption of Au NPs in the reaction solution (obtained by subtracting the contribution of pure TiO_2 absorption from the absorption of Au/TiO_2 samples), and the inset image is the photograph of the Au NPs solution.

photoexcited electrons with a more negative potential at the Au NPs, they can inject into the conduction band of TiO_2 and trigger photoreaction [39, 58, 59]. Besides, the LSPR-absorption of Au NPs may activate TiO_2 to generate photoexcited electrons and holes directly under visible light irradiation [39, 60].

On the basis of above results, we believe that the overlapped light harvesting nanostructures of Au/TiO_2 films play an important role in the improved visible light photoactivity. The LSPR-absorption of Au NPs on the surface of TiO_2 film can give valid evidence, which exhibits a broad response ranging from 350 nm to 750 nm with two peaks at 389 nm and 540 nm in Figure 9(a). It is different to the narrow LSPR-absorption of Au NPs in the solution (Figure 9(b)). This is because Au NPs and TiO_2 film are responsive to visible light simultaneously, and the incident light captured by TiO_2 film is overlapped with the LSPR-absorption of Au NPs in the visible light range. This overlapped harvesting phenomenon suggests a strong interaction between Au NPs and TiO_2 film and implies that they can work as a visible-light-driven photocatalyst. The absorption peak at 389 nm may be related to the bang gap of anatase TiO_2, which shows a clear absorption edge shorter than 390 nm. The light (λ < 390 nm) captured by TiO_2 film can be used to generate charge carriers, and the rest of the captured light (λ > 390 nm) can be reused by Au NPs due to the overlapped light harvesting nanostructures, leading to an enhanced LSPR-absorption (Figure 9(a)). Therefore, the improved optical overlap between the absorptions of TiO_2 film and Au NPs is the main cause for the enhanced LSPR-absorption of Au NPs. The enhanced light absorption in the visible light region can improve the activity of TiO_2 by increasing the quantities of photoexcited charge carriers or by enhancing the energy of trapped electron.

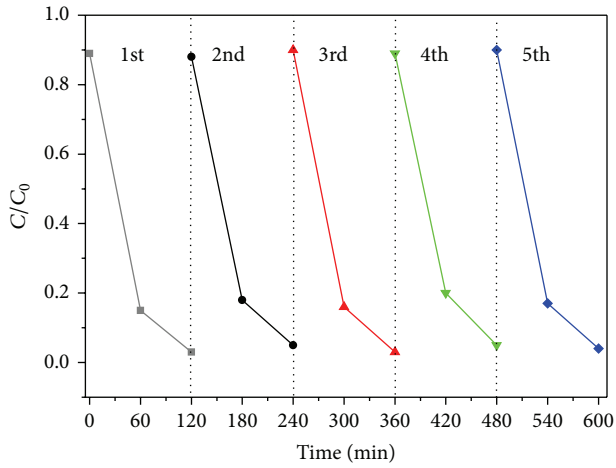

Figure 10: Cycling runs for five times in the photocatalytic degradation of MB over 0.6 Au/TiO_2 film.

The stability of the photocatalysts is essential to the practical applications. The photocatalytic stability of the 0.6 Au/TiO_2 film was evaluated by cycling degradation experiments and the corresponding results are shown in Figure 10. It can be seen clearly that 0.6 Au/TiO_2 film maintains an efficient and stable photocatalytic activity even after five cycles. The XPS spectra shown in Figure 4 indicate that there is an inappreciable change of the chemical state and the content of Au nanoparticles in the composite before and after cycling

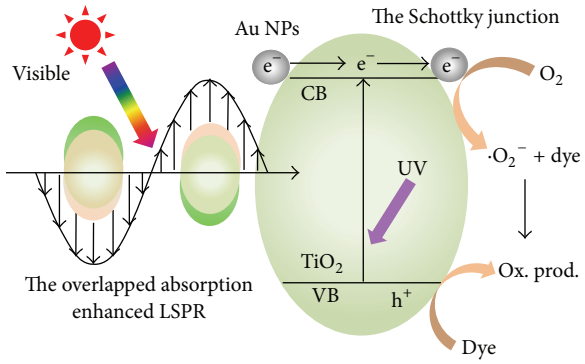

Figure 11: Schematic illustration of photocatalytic degradation of MB over Au/TiO_2 composite with overlapped light harvesting nanostructures.

photodegradation experiments. All these analyses indicate that Au/TiO_2 film possesses high activity and stability.

3.3. The Enhancement Mechanism of Photocatalytic Degradation of MB. A tentative photocatalytic mechanism is proposed and schematically illustrated in Figure 11. (i) Under UV light irritation, the Schottky junction between Au NPs and TiO_2 can facilitate charge separation, leading to an enhanced photocatalytic activity. (ii) Under visible light irritation, on the one hand, LSPR-induced electrons in Au NPs can transfer from Au NPs to TiO_2 and trigger photoreaction. On the other hand, the LSPR effect of Au NPs is induced by the visible light, forming a strong local electronic field to enhance the energy of trapped electrons, making them transfer and react with electron acceptors more easily. In any case, the enhanced LSPR-absorption is positive for the photocatalytic process. (iii) Overlapped light harvesting nanostructures can provide a strong interaction between Au NPs and TiO_2 film, and visible light trapped by TiO_2 can be reused by Au NPs, leading to an enhanced LSPR-absorption. Besides, the overlapped absorption may be also beneficial for the MB photosensitization. Based on what has been observed and discussed above, it is reasonable to conclude that the enhanced photocatalytic activity could be attributed to the charge transfer property of Au NPs and the efficient light utilization based on the overlapped light harvesting nanostructures of composite film. As shown in Figure 6(b), the highest MB degradation rate is obtained under UV and visible light irradiations, which results from the synergetic effect between charge transfer and overlapped light harvesting properties in Au/TiO_2 composite.

4. Conclusion

A novel visible light responsive plasmonic Au/TiO_2 films with two dimensional nanosheet structures were successfully fabricated by the combination of a hydrothermal process and a microwave-assisted reduction route. The prepared samples exhibit an obviously overlapped light absorption due to the localized surface plasmon resonance of Au NPs and unique nanostructures of TiO_2 film. The light trapped by TiO_2 nanosheet film can be reused by the LSPR of Au NPs. The MB degradation over 0.6 Au/TiO_2 film is much faster than that of pure TiO_2 film by a factor of 5.7 under UV light and visible light irradiations. The improved activity of Au/TiO_2 composite is ascribed to the changer transfer property of Au NPs and the overlapped light harvesting nanostructures. A synergy between charge transfer and overlapped absorption can greatly enhance the degradation efficiency of MB. This study suggests a simple strategy to develop LSPR-enhanced photocatalysis systems with film-shaped nanostrucutres and high efficiency.

Conflict of Interests

The authors declare that there is no conflict of interests regarding the publication of this paper.

Acknowledgments

This work was financially supported by the College Students Innovative Entrepreneurial Training Program (2015202), the National Natural Science Foundation of China (21306150, 21176199, 21476183, and 51372201), the Specialized Research Fund for the Doctoral Program of Higher Education of China (20136101110009), the Shaanxi Provincial Research Foundation for Basic Research (2013JQ2003), the Scientific Research Foundation of Education Department of Shaanxi Provincial Government (2013JK0693), the Scientific Research Foundation of Northwest University (12NW19), and the Scientific Research Staring Foundation of Northwest University (PR12216).

References

[1] A. Fujishima and K. Honda, "Photolysis-decomposition of water at the surface of an irradiated semiconductor," *Nature*, vol. 238, pp. 37–38, 1972.

[2] J. Liu, Y. Liu, N. Liu et al., "Metal-free efficient photocatalyst for stable visible water splitting via a two-electron pathway," *Science*, vol. 347, no. 6225, pp. 970–974, 2015.

[3] M. Tokarčíková, J. Tokarský, K. Čabanová, V. Matějka, K. M. Kutláková, and J. Seidlerová, "The stability of photoactive kaolinite/TiO_2 composite," *Composites Part B: Engineering*, vol. 67, pp. 262–269, 2014.

[4] W. Fan, Q. Zhang, and Y. Wang, "Semiconductor-based nanocomposites for photocatalytic H_2 production and CO_2 conversion," *Physical Chemistry Chemical Physics*, vol. 15, no. 8, pp. 2632–2649, 2013.

[5] X. Li, J. Yu, J. Low, Y. Fang, J. Xiao, and X. Chen, "Engineering heterogeneous semiconductors for solar water splitting," *Journal of Materials Chemistry A*, vol. 3, no. 6, pp. 2485–2534, 2015.

[6] J. Ran, J. Zhang, J. Yu, M. Jaroniec, and S. Z. Qiao, "Earth-abundant cocatalysts for semiconductor-based photocatalytic water splitting," *Chemical Society Reviews*, vol. 43, no. 22, pp. 7787–7812, 2014.

[7] X. Li, J. Wen, J. Low, Y. Fang, and J. Yu, "Design and fabrication of semiconductor photocatalyst for photocatalytic reduction of CO_2 to solar fuel," *Science China Materials*, vol. 57, no. 1, pp. 70–100, 2014.

[8] R. Asai, H. Nemoto, Q. Jia, K. Saito, A. Iwase, and A. Kudo, "A visible light responsive rhodium and antimony-codoped

$SrTiO_3$ powdered photocatalyst loaded with an IrO_2 cocatalyst for solar water splitting," *Chemical Communications*, vol. 50, no. 19, pp. 2543–2546, 2014.

[9] Y. Yang, E. Liu, H. Dai et al., "Photocatalytic activity of Ag-TiO_2-graphene ternary nanocomposites and application in hydrogen evolution by water splitting," *International Journal of Hydrogen Energy*, vol. 39, no. 15, pp. 7664–7671, 2014.

[10] X. Zhou, Y. Liu, X. Li, Q. Gao, X. Liu, and Y. Fang, "Topological morphology conversion towards SnO_2/SiC hollow sphere nanochains with efficient photocatalytic hydrogen evolution," *Chemical Communications*, vol. 50, no. 9, pp. 1070–1073, 2014.

[11] Q. Xiang, J. Yu, and M. Jaroniec, "Preparation and enhanced visible-light photocatalytic H_2 production activity of graphene/C_3N_4 composites," *Journal of Physical Chemistry C*, vol. 115, no. 15, pp. 7355–7363, 2011.

[12] J. Yuan, J. Wen, Q. Gao et al., "Amorphous Co_3O_4 modified CdS nanorods with enhanced visible-light photocatalytic H_2 production activity ," *Dalton Transactions*, vol. 44, no. 4, pp. 1680–1689, 2015.

[13] Y. Li, H. Gou, J. Lu, and C. Wang, "A two-step synthesis of $NaTaO_3$ microspheres for photocatalytic water splitting," *International Journal of Hydrogen Energy*, vol. 39, pp. 13481–13485, 2014.

[14] J. Wan, E. Liu, J. Fan et al., "In-situ synthesis of plasmonic Ag/Ag_3PO_4 tetrahedron with exposed 111 facets for high visible-light photocatalytic activity and stability," *Ceramics International*, vol. 41, no. 5, pp. 6933–6940, 2015.

[15] S. Ko, C. K. Banerjee, and J. Sankar, "Photochemical synthesis and photocatalytic activity in simulated solar light of nanosized Ag doped TiO_2 nanoparticle composite," *Composites Part B: Engineering*, vol. 42, no. 3, pp. 579–583, 2011.

[16] W. J. Youngblood, S.-H. A. Lee, K. Maeda, and T. E. Mallouk, "Visible light water splitting using dye-sensitized oxide semiconductors," *Accounts of Chemical Research*, vol. 42, no. 12, pp. 1966–1973, 2009.

[17] X. Li, T. Xia, C. Xu, J. Murowchick, and X. Chen, "Synthesis and photoactivity of nanostructured CdS-TiO_2 composite catalysts," *Catalysis Today*, vol. 225, pp. 64–73, 2014.

[18] X. Fan, J. Fan, X. Y. Hu et al., "Preparation and characterization of Ag deposited and Fe doped TiO_2 nanotube arrays for photocatalytic hydrogen production by water splitting," *Ceramics International*, vol. 40, no. 10, pp. 15907–15917, 2014.

[19] C. Tang, E. Liu, J. Fan, X. Hu, L. Kang, and J. Wan, "Heterostructured Ag_3PO_4/TiO_2 nano-sheet film with high efficiency for photodegradation of methylene blue," *Ceramics International*, vol. 40, no. 10, pp. 15447–15453, 2014.

[20] Q. Xiang, J. Yu, and M. Jaroniec, "Synergetic effect of MoS_2 and graphene as cocatalysts for enhanced photocatalytic H_2 production activity of TiO_2 nanoparticles," *Journal of the American Chemical Society*, vol. 134, no. 15, pp. 6575–6578, 2012.

[21] X. Yue, J. Zhang, F. Yan, X. Wang, and F. Huang, "A situ hydrothermal synthesis of $SrTiO_3$/TiO_2 heterostructure nanosheets with exposed (001) facets for enhancing photocatalytic degradation activity," *Applied Surface Science*, vol. 319, pp. 68–74, 2014.

[22] W. Wang, Y. Ni, C. Lu, and Z. Xu, "Hydrogenation temperature related inner structures and visible-light-driven photocatalysis of N-F co-doped TiO_2 nanosheets," *Applied Surface Science*, vol. 290, pp. 125–130, 2014.

[23] J. Puskelova, R. Michal, M. Caplovicova et al., "Hydrogen production by photocatalytic ethanol reforming using Eu- and S-doped anatase," *Applied Surface Science*, vol. 305, pp. 665–669, 2014.

[24] X. Li, H. Liu, D. Luo et al., "Adsorption of CO_2 on heterostructure CdS(Bi_2S_3)/TiO_2 nanotube photocatalysts and their photocatalytic activities in the reduction of CO_2 to methanol under visible light irradiation," *Chemical Engineering Journal*, vol. 180, pp. 151–158, 2012.

[25] J. Yu, J. Low, W. Xiao, P. Zhou, and M. Jaroniec, "Enhanced photocatalytic CO_2-reduction activity of anatase TiO_2 by coexposed {001} and {101} facets," *Journal of the American Chemical Society*, vol. 136, no. 25, pp. 8839–8842, 2014.

[26] J. Zhang, S. Yan, S. Zhao, Q. Xu, and C. Li, "Photocatalytic activity for H_2 evolution of TiO_2 with tuned surface crystalline phase," *Applied Surface Science*, vol. 280, pp. 304–311, 2013.

[27] F. Xu, W. Xiao, B. Cheng, and J. Yu, "Direct Z-scheme anatase/rutile bi-phase nanocomposite TiO_2 nanofiber photocatalyst with enhanced photocatalytic H_2-production activity," *International Journal of Hydrogen Energy*, vol. 39, no. 28, pp. 15394–15402, 2014.

[28] J.-D. Lin, S. Yan, Q.-D. Huang et al., "TiO_2 promoted by two different non-noble metal cocatalysts for enhanced photocatalytic H_2 evolution," *Applied Surface Science*, vol. 309, pp. 188–193, 2014.

[29] K. Awazu, M. Fujimaki, C. Rockstuhl et al., "A plasmonic photocatalyst consisting of silver nanoparticles embedded in titanium dioxide," *Journal of the American Chemical Society*, vol. 130, no. 5, pp. 1676–1680, 2008.

[30] C. Clavero, "Plasmon-induced hot-electron generation at nanoparticle/metal-oxide interfaces for photovoltaic and photocatalytic devices," *Nature Photonics*, vol. 8, no. 2, pp. 95–103, 2014.

[31] S. Linic, P. Christopher, and D. B. Ingram, "Plasmonic-metal nanostructures for efficient conversion of solar to chemical energy," *Nature Materials*, vol. 10, no. 12, pp. 911–921, 2011.

[32] P. Wang, B. Huang, Y. Dai, and M.-H. Whangbo, "Plasmonic photocatalysts: harvesting visible light with noble metal nanoparticles," *Physical Chemistry Chemical Physics*, vol. 14, no. 28, pp. 9813–9825, 2012.

[33] X. Zhou, G. Liu, J. Yu, and W. Fan, "Surface plasmon resonance-mediated photocatalysis by noble metal-based composites under visible light," *Journal of Materials Chemistry*, vol. 22, no. 40, pp. 21337–21354, 2012.

[34] A. Bumajdad and M. Madkour, "Understanding the superior photocatalytic activity of noble metals modified titania under UV and visible light irradiation," *Physical Chemistry Chemical Physics*, vol. 16, no. 16, pp. 7146–7158, 2014.

[35] E. Liu, Y. Hu, H. Li et al., "Photoconversion of CO_2 to methanol over plasmonic Ag/TiO_2 nano-wire films enhanced by overlapped visible-light-harvesting nanostructures," *Ceramics International*, vol. 41, no. 1, pp. 1049–1057, 2015.

[36] Y. Wang, J. Yu, W. Xiao, and Q. Li, "Microwave-assisted hydrothermal synthesis of graphene based Au-TiO_2 photocatalysts for efficient visible-light hydrogen production," *Journal of Materials Chemistry A*, vol. 2, no. 11, pp. 3847–3855, 2014.

[37] A. Ramchiary and S. K. Samdarshi, "Ag deposited mixed phase titania visible light photocatalyst-superiority of Ag-titania and mixed phase titania co-junction," *Applied Surface Science*, vol. 305, pp. 33–39, 2014.

[38] Z. Liu, W. Hou, P. Pavaskar, M. Aykol, and S. B. Cronin, "Plasmon resonant enhancement of photocatalytic water splitting under visible illumination," *Nano Letters*, vol. 11, no. 3, pp. 1111–1116, 2011.

[39] X. Zhang, Y. L. Chen, R. S. Liu, and D. P. Tsai, "Plasmonic photocatalysis," *Reports on Progress in Physics*, vol. 76, no. 4, Article ID 046401, 2013.

[40] D. Jose, C. M. Sorensen, S. S. Rayalu, K. M. Shrestha, and K. J. Klabunde, "Au-TiO_2 nanocomposites and efficient photocatalytic hydrogen production under UV-visible and visible light illuminations: a comparison of different crystalline forms of TiO_2," *International Journal of Photoenergy*, vol. 2013, Article ID 685614, 10 pages, 2013.

[41] D. B. Ingram, P. Christopher, J. L. Bauer, and S. Linic, "Predictive model for the design of plasmonic metal/semiconductor composite photocatalysts," *ACS Catalysis*, vol. 1, no. 10, pp. 1441–1447, 2011.

[42] W. Hou, Z. Liu, P. Pavaskar, W. H. Hung, and S. B. Cronin, "Plasmonic enhancement of photocatalytic decomposition of methyl orange under visible light," *Journal of Catalysis*, vol. 277, no. 2, pp. 149–153, 2011.

[43] H. Gao, C. Liu, H. E. Jeong, and P. Yang, "Plasmon-enhanced photocatalytic activity of iron oxide on gold nanopillars," *ACS Nano*, vol. 6, no. 1, pp. 234–240, 2012.

[44] E. Liu, L. Kang, Y. Yang et al., "Plasmonic Ag deposited TiO_2 nano-sheet film for enhanced photocatalytic hydrogen production by water splitting," *Nanotechnology*, vol. 25, no. 16, Article ID 165401, 2014.

[45] E. Liu, J. Fan, X. Hu et al., "A facile strategy to fabricate plasmonic Au/TiO_2 nano-grass films with overlapping visible light-harvesting structures for H_2 production from water," *Journal of Materials Science*, vol. 50, no. 5, pp. 2298–2305, 2015.

[46] S. Zhang, F. Peng, H. Wang, H. Yu, J. Yang, and H. Zhao, "Electrodeposition preparation of Ag loaded N-doped TiO_2 nanotube arrays with enhanced visible light photocatalytic performance," *Catalysis Communications*, vol. 12, no. 8, pp. 689–693, 2011.

[47] Y. Wu, H. Liu, J. Zhang, and F. Chen, "Enhanced photocatalytic activity of nitrogen-doped titania by deposited with gold," *Journal of Physical Chemistry C*, vol. 113, no. 33, pp. 14689–14695, 2009.

[48] J.-G. Yu, H.-G. Yu, B. Cheng, X.-J. Zhao, J. C. Yu, and W.-K. Ho, "The effect of calcination temperature on the surface microstructure and photocatalytic activity of TiO_2 thin films prepared by liquid phase deposition," *Journal of Physical Chemistry B*, vol. 107, no. 50, pp. 13871–13879, 2003.

[49] J. Yu, X. Zhao, and Q. Zhao, "Effect of surface structure on photocatalytic activity of TiO_2 thin films prepared by sol-gel method," *Thin Solid Films*, vol. 379, no. 1-2, pp. 7–14, 2000.

[50] H. Zhu, B. Yang, J. Xu et al., "Construction of Z-scheme type CdS-Au-TiO_2 hollow nanorod arrays with enhanced photocatalytic activity," *Applied Catalysis B: Environmental*, vol. 90, no. 3-4, pp. 463–469, 2009.

[51] A. R. Hernandez-Martinez, M. Estevez, S. Vargas, and R. Rodriguez, "New polyurethane-anatase titania porous hybrid composite for the degradation of azo-compounds wastes," *Composites Part B: Engineering*, vol. 44, no. 1, pp. 686–691, 2013.

[52] J. A. O. Méndez, C. R. López, E. P. Melián et al., "Production of hydrogen by water photo-splitting over commercial and synthesised Au/TiO_2 catalysts," *Applied Catalysis B: Environmental*, vol. 147, pp. 439–452, 2014.

[53] A. Ramchiary and S. K. Samdarshi, "Ag deposited mixed phase titania visible light photocatalyst—superiority of Ag-titania and mixed phase titania co-junction," *Applied Surface Science*, vol. 305, pp. 33–39, 2014.

[54] X. He, Y. Cai, H. Zhang, and C. Liang, "Photocatalytic degradation of organic pollutants with Ag decorated free-standing TiO_2 nanotube arrays and interface electrochemical response," *Journal of Materials Chemistry*, vol. 21, no. 2, pp. 475–480, 2011.

[55] Y. Koo, G. Littlejohn, B. Collins et al., "Synthesis and characterization of Ag-TiO_2-CNT nanoparticle composites with high photocatalytic activity under artificial light," *Composites Part B: Engineering*, vol. 57, pp. 105–111, 2014.

[56] S. Zhang, B. Peng, S. Yang et al., "Non-noble metal copper nanoparticles-decorated TiO_2 nanotube arrays with plasmon-enhanced photocatalytic hydrogen evolution under visible light," *International Journal of Hydrogen Energy*, vol. 40, no. 1, pp. 303–310, 2015.

[57] S. Zhang, B. Peng, S. Yang, Y. Fang, and F. Peng, "The influence of the electrodeposition potential on the morphology of Cu_2O/TiO_2 nanotube arrays and their visible-light-driven photocatalytic activity for hydrogen evolution," *International Journal of Hydrogen Energy*, vol. 38, no. 32, pp. 13866–13871, 2013.

[58] H. Li, X. Duan, G. Liu, and X. Liu, "Photochemical synthesis and characterization of Ag/TiO_2 nanotube composites," *Journal of Materials Science*, vol. 43, no. 5, pp. 1669–1676, 2008.

[59] Y. Wen, B. Liu, W. Zeng, and Y. Wang, "Plasmonic photocatalysis properties of Au nanoparticles precipitated anatase/rutile mixed TiO_2 nanotubes," *Nanoscale*, vol. 5, no. 20, pp. 9739–9746, 2013.

[60] Y.-R. He, F.-F. Yan, H.-Q. Yu, S.-J. Yuan, Z.-H. Tong, and G.-P. Sheng, "Hydrogen production in a light-driven photoelectrochemical cell," *Applied Energy*, vol. 113, pp. 164–168, 2014.